A Mixed Finite Element Method for 3-D Analysis of Cavity Resonators

By Fumio KIKUCHI,[1] Masahiro HARA[2] and Takeshi WADA[2]

1. Department of Mathematics, College of Arts and Sciences, University of Tokyo,
2. Institute of Physical and Chemical Research, 2-1 Hirosawa, Wako-shi, Saitama, 351-01

(Received February 3, 1992)

Abstract

This paper presents a finite element method for 3-D analysis of an electromagnetic eigenvalue problem for cavity resonators. First, we derive some weak formulations for this problem, a typical one of which is a mixed formulation that employs the Lagrange multiplier to deal with the divergence-free condition. Then we give a mixed finite element method based on the mixed formulation. We present concrete finite element models by the use of the Nedelec type finite element spaces for electric or magnetic fields. This approach is mathematically rigorous and is also convenient to deal with the electromagnetic boundary conditions. We also present some finite element models for the analysis of axisymmetric cavities. Finally, some elementary numerical results are given to demonstrate the validity of our approach.

Key words: eigenvalue problem, electromagnetics, mixed FEM, Nedelec edge elements

§ 1. Introduction

In 3-D (three-dimensional) analysis of cavity resonators, we have the following eigenvalue problem for the electric field $\vec{E}$ [1]:

$$\mathrm{rot}\,\mathrm{rot}\,\vec{E}=\lambda\vec{E},\ \mathrm{div}\,\vec{E}=0 \text{ in } \Omega;\quad \vec{n}\times\vec{E}=\vec{0} \text{ on } \partial\Omega\,, \tag{1}$$

where λ is the eigenvalue that is proportional to the square of frequency, Ω is a bounded 3-D domain occupied by the cavity, $\times$ denotes the outer product operation, $\partial\Omega$ is the boundary of Ω, and $\vec{n}$ is the unit outward normal on $\partial\Omega$. Sometimes, a boundary condition $\mathrm{div}\,\vec{E}=0$ is supplemented on $\partial\Omega$. If we use the magnetic field $\vec{H}$ in place of $\vec{E}$, the problem becomes

$$\mathrm{rot}\,\mathrm{rot}\,\vec{H}=\lambda\vec{H},\ \mathrm{div}\,\vec{H}=0 \text{ in } \Omega;\quad \vec{n}\cdot\vec{H}=0,\ \vec{n}\times\mathrm{rot}\,\vec{H}=\vec{0} \text{ on } \partial\Omega\,, \tag{2}$$

where $\cdot$ denotes the inner product operation. It has been very difficult to apply

the finite element method to 3-D analysis of the above problem probably for lack of appropriate weak (or variational) formulations and reliable finite element models.

In this paper, we will present weak formulations for the above problem, including a mixed formulation based on the Lagrange multiplier method. Some comments are also given on artificial boundary conditions for problems with geometric symmetry and/or antisymmetry. Then we will give a new family of mixed finite element models by the use of the Nedelec finite element spaces for $\vec{E}$ or $\vec{H}$ [17, 18]. In this approach, the nodes of elements are edges, and the nodal unknowns (degrees of freedom) are the values of $\vec{E}$ or $\vec{H}$ in the edge directions. Hence, such elements are also called *edge elements*. The assumed distributions of $\vec{E}$ or $\vec{H}$ are queer-looking low order polynomials that are discontinuous on interelement boundaries but whose tangential components are continuous. These elements are also very easy to deal with the boundary conditions appearing in (1) or (2). We will also give some comments on the properties of the arising algebraic eigenvalue problems in the finite element analysis. In particular, the Lagrange multiplier may be eliminated in numerical computations at the expense of getting highly degenerated zero eigenvalue in the approximate problem. Thus, when such elimination is made, we must be very careful to separate physically meaningful (positive) eigenvalues from such nonphysical (spurious) one. We have developed computer programs and obtain some numerical results to demonstrate the feasibility of our approach. We also test performances of some existing supercomputers by our computer programs. The results are generally reasonable, and the proposed approach appears to be very promising. For theoretical analysis of the method, see Kikuchi [11, 12, 13]. In Appendix, we give explicit expressions for several kinds of approximate functions for $\vec{E}$ or $\vec{H}$.

Before going into our main subjects, we list some important works related to ours. Weiland [19] developed a finite difference scheme based on the control volume method, which is similar to our finite element schemes. He also applied the scheme to analysis of cavities of various shapes. As is already mentioned, Nedelec [17, 18] proposed some finite elements for approximating vector fields with their rotations. He also analyzed approximation properties of the proposed elements. Hano [8] presented a rectangular finite element independently of Nedelec, and applied it to two-dimensional cavity resonator problems (i.e., the waveguide problems). Bossavit [3] also showed that the Nedelec elements can be applied to numerical analysis of various electromagnetic problems. Furthermore, he pointed out that such finite elements can be traced back to Whitney [20], and named them the Whitney elements. Our work started independently of these related ones, but has been much refined thanks to them. It is also to be pointed out that Krizek and Neittaanmaki [15] made clear that the classical vertex type finite elements may be used to the present problem if Ω has sufficiently smooth boundary. However, such an approach is inadequate, for example, when Ω has a reentrant corner [12].

§ 2. Basic formulations

Let Ω be a bounded domain in $\boldsymbol{R}^3$ with Lipschitz continuous boundary $\partial\Omega$. The explanations given below are valid for the two-dimensional (2-D) problems corresponding to (1) and (2) after minor modifications.

Let $L_2(\Omega)$, $H^1(\Omega)$ and $H_0(\Omega)$ be the usual (real) L_2-type Hilbert spaces of functions defined in Ω, and let us denote the inner products of $L_2(\Omega)$ and $L_2(\Omega)^3$ by the common notation $(\cdot, \cdot)$. We also use the following real Hilbert spaces appearing in electromagnetics [5, 6].

$$H(\mathrm{rot}, \Omega)=\{\vec{E}\in L_2(\Omega)^3;\ \mathrm{rot}\,\vec{E}\in L_2(\Omega)^3\}\ , \tag{3}$$

$$H_0(\mathrm{rot}, \Omega)=\{\vec{E}\in H(\mathrm{rot}, \Omega):\ \vec{n}\times\vec{E}=\vec{0}\ \text{on}\ \partial\Omega\}\ . \tag{4}$$

The second space above is used for electric fields since the tangential components of functions in this space vanish on $\partial\Omega$. Hereafter, we will summarize some weak (or variational) formulations for (1) and (2) derived by one of the present authors [11, 12]. There are some other related formulations which are not presented below, since they are not explicitly used in this paper.

First, let us show some weak formulations in terms of electric field $\vec{E}$. A natural weak formulation for (1) is:

[E1]. *Find* $\{\lambda, \vec{E}\}\in \boldsymbol{R}^1\times H_0(\mathrm{rot}, \Omega)$ *such that* $\vec{E}\neq\vec{0}$ *and*

$$(\mathrm{rot}\,\vec{E},\ \mathrm{rot}\,\vec{E}^*)=\lambda(\vec{E}, \vec{E}^*);\quad \forall\vec{E}^*\in H_0(\mathrm{rot}, \Omega)\ , \tag{5-1}$$

$$(\vec{E},\ \mathrm{grad}\,q)=0\quad \forall q\in H_0^1(\Omega)\ . \tag{5-2}$$

Here, (5-2) simply means that $\mathrm{div}\,\vec{E}=0$ in the distributional sense. Note here that if $\vec{E}$ satisfies (5-1) for $\lambda\neq 0$, then it also satisfies (5-2) since we can substitute $\mathrm{grad}\,q$ as $\vec{E}^*$ into (5-1). Thus, we can omit (5-2) in purely theoretical considerations. However, such an approach is often accompanied with the *spectral pollution* in practical numerical computations [7], since $\lambda=0$ then becomes an infinitely degenerate eigenvalue.

To deal with (5-2) more rigorously, we consider the following mixed formulation based on the Lagrange multiplier method.

[E2]. *Find* $\{\lambda, \vec{E}, p\}\in \boldsymbol{R}^1\times H_0(\mathrm{rot}, \Omega)\times H_0^1(\Omega)$ *such that* $\vec{E}\neq\vec{0}$ *and*

$$(\mathrm{rot}\,\vec{E},\ \mathrm{rot}\,\vec{E}^*)+(\mathrm{grad}\,p,\ \vec{E}^*)=\lambda(\vec{E}, \vec{E}^*);\quad \forall\vec{E}^*\in H_0(\mathrm{rot}, \Omega)\ , \tag{6-1}$$

$$(\vec{E},\ \mathrm{grad}\,q)=0;\quad \forall q\in H_0^1(\Omega)\ . \tag{6-2}$$

The Lagrange multiplier is p, which is shown to be zero by equating $\vec{E}^*$ to $\mathrm{grad}\,p\in H_0(\mathrm{rot}, \Omega)$ in (6-1).

If we use the magnetic field $\vec{H}$ in place of the electric field, we have the following weak formulations for (2).

[H1]. *Find* $\{\lambda, \vec{H}\}\in \boldsymbol{R}^1\times H(\mathrm{rot}, \Omega)$ *such that* $\vec{H}\neq\vec{0}$ *and*

$$(\mathrm{rot}\,\vec{H}, \mathrm{rot}\,\vec{H}^*)=\lambda(\vec{H}, \vec{H}^*); \quad \forall\vec{H}^* \in H(\mathrm{rot}, \Omega)\ , \tag{7-1}$$

$$(\vec{H}, \mathrm{grad}\,q)=0; \quad \forall q \in H^1(\Omega)\ . \tag{7-2}$$

[H2]. *Find* $\{\lambda, \vec{H}, p) \in \boldsymbol{R}^1 \times (\mathrm{rot}, \Omega) \times H^1(\Omega)$ *such that* $\vec{H} \neq \vec{0}$ *and*

$$(\mathrm{rot}\,\vec{H}, \mathrm{rot}\,\vec{H}^*)+(\mathrm{grad}\,p, \vec{H}^*)=\lambda(\vec{H}, \vec{H}^*); \quad \forall\vec{H}^* \in H(\mathrm{rot}, \Omega)\ , \tag{8-1}$$

$$(\vec{H}, \mathrm{grad}\,q)=0; \quad \forall q \in H^1(\Omega)\ . \tag{8-2}$$

Note the difference of the employed function spaces from those of [E1] and [E2]. Again, the Lagrange multiplier becomes zero (more precisely, $\mathrm{grad}\,p=0$). The boundary conditions in (2) are now taken into account either as a natural boundary condition or a constraint condition in the present two formulations, and do not appear explicitly in the requirements for the employed function spaces $H(\mathrm{rot}, \Omega)$ and $H^1(\Omega)$. Equivalence of [H2] to [E2] for $\lambda \neq 0$ is fully discussed in [12] in the framework of L_2-theory.

§ 3. Finite element models

We will consider a mixed finite element method based on [E2]. It is also possible to construct a finite element method based on [H2] if we modify the boundary conditions imposed on the approximate function spaces.

Hereafter, we assume Ω to to be a bounded polyhedral domain for simplicity. We first consider a regular family of triangulations for Ω by tetrahedra and then construct an appropriate family of finite-dimensional subspaces of $H_0(\mathrm{rot}, \Omega) \times H_0^1(\Omega)$ associated with the triangulations.

After Nedelec [17, 18], we approximate $\vec{E}=\{E_x, E_y, E_z\}$ in each tetrahedron finite element (Fig. 1) as

$$E_x=\alpha_1+\alpha_2 y+\alpha_3 z,\ E_y=\alpha_4-\alpha_2 x+\alpha_5 z,\ E_z=\alpha_6-\alpha_3 x-\alpha_5 y\ , \tag{9}$$

where $\alpha_1, \cdots, \alpha_6$ are coefficients, and x, y and z are the usual Cartesian coordinate components. Furthermore, we impose that the tangential components of the above $\vec{E}$ are continuous on the common face of any two tetrahedra in

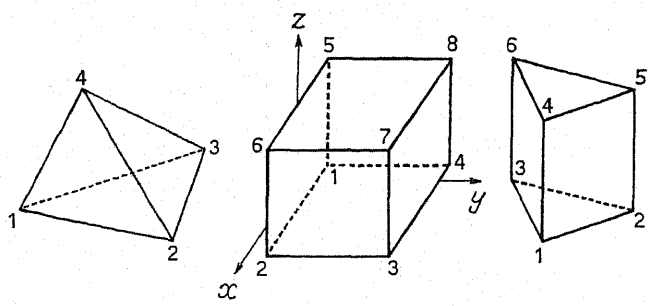

Fig. 1. 3-D edge elements with vertex numberings

the triangulation. Then the totality of such fields is shown to be a finite-dimensional subspace of $H(\mathrm{rot}, \Omega)$, which we will denote by X^h. If we also impose on $\vec{E}$ that its tangential components vanish on $\partial\Omega$, then the totality of such functions becomes a finite dimensional subspace of $H_0(\mathrm{rot}, \Omega)$. We will denote it by X_0^h. In the present approximation, the "nodes" of finite elements are edges, and the nodal parameters (degrees of freedom) are the components of $\vec{E}$ in the edge directions, which are shown to be constant. Moreover, such $\vec{E}$ satisfies that $\mathrm{rot}\,\vec{E}=\mathrm{const.}$ and $\mathrm{div}\,\vec{E}=0$ in each tetrahedron.

On the other hand, the approximation of p is the usual piecewise linear polynomial, that is,

$$p=\beta_1+\beta_2 x+\beta_3 y+\beta_4 z \quad \text{in each tetrahedron}\,. \tag{10}$$

Moreover, p is continuous on all interfaces between tetrahedra. Then the totality of such p is a finite-dimensional subspace of $H^1(\Omega)$, which we will denote by Y^h. If p vanishes on $\partial\Omega$ in addition, then the totality of such p is a finite-dimensional subspace of $H_0^1(\Omega)$, which we will denote by Y_0^h. An important relation to hold between X^h and Y^h (X_0^h and Y_0^h, resp.) is:

$$\mathrm{grad}\,p_h \in X^h;\ \forall p_h \in Y^h \quad (\mathrm{grad}\,p_h \in X_0^h;\ \forall p_h \in Y_0^h,\ \text{resp.})\,. \tag{11}$$

The mixed finite element method based on [E2] is as follows.

$[\mathbf{E2}]_h$. *Find* $\{\lambda_h, \vec{E}_h, p_h\} \in \boldsymbol{R}^1 \times X_0^h \times Y_0^h$ *such that* $\vec{E}_h \neq \vec{0}$ *and*

$$(\mathrm{rot}\,\vec{E}_h, \mathrm{rot}\,\vec{E}_h^*)+(\mathrm{grad}\,p_h, \vec{E}_h^*)=\lambda_h(\vec{E}_h, \vec{E}_h^*);\quad \forall \vec{E}_h^* \in X_0^h\,, \tag{12-1}$$

$$(\vec{E}_h, \mathrm{grad}\,q_h)=0;\quad \forall q_h \in Y_0^h\,. \tag{12-2}$$

Thanks to (11), we find that $p_h=0$ by equating $\vec{E}_h^*=\mathrm{grad}\,p_h$ in (12). Moreover, substituting $p_h=0$ into (12), we have the following approximate problem corresponding to [E1].

$[\mathbf{E1}]_h$. *Find* $\{\lambda_h, \vec{E}_h\} \in \boldsymbol{R}^1 \times X_0^h$ *such that* $\vec{E}_h \neq \vec{0}$ *and*

$$(\mathrm{rot}\,\vec{E}_h, \mathrm{rot}\,\vec{E}_h^*)=\lambda_h(\vec{E}_h, \vec{E}_h^*);\quad \forall \vec{E}_h^* \in X_0^h\,, \tag{13-1}$$

$$(\vec{E}_h, \mathrm{grad}\,q_h)=0;\quad \forall q_h \in Y_0^h\,. \tag{13-2}$$

Again by (11), we find that $\vec{E}_h \in X_0^h$ satisfying the first relation of (13) for $\lambda_h \neq 0$ satisfies the second one as well. Thus, in the present finite element scheme, it is sufficient to deal with the first relation of (13) only, so long as we consider non-zero approximate eigenvalues only. This is practically reasonable since the zero eigenvalue is usually unnecessary to obtain.

From the observations above, we will solve numerically the following approximate eigenvalue problem for the pair $\{\lambda_h, \vec{E}_h\} \in \boldsymbol{R}^1 \times X_0^h$:

$$(\mathrm{rot}\,\vec{E}_h, \mathrm{rot}\,\vec{E}_h^*)=\lambda_h(\vec{E}_h, \vec{E}_h^*);\quad \forall \vec{E}_h^* \in X_0^h\,. \tag{14}$$

Based on (14), we can obtain the element matrices by the standard procedure

of the finite element method [2]. In the present case, the integrations required in this process can be done explicitly by using the expressions of shape functions. The algebraic eigenvalue problem thus obtained is of course a matrix eigenvalue problem, for which, for example, the inverse iteration method and the subspace iteration method are available [2]. However, an important fact to note is that the zero eigenvalue is usually highly degenerate, and we must be very careful to separate the desired (i.e., non-zero) eigenvalues from the zero eigenvalue. To this end, the shift techniques appear to be well suited [2]. When $\partial\Omega$ is connected as is usually the case with cavity resonators, the eigenspace associated with the zero eigenvalue of (14) is explicitly given by

$$\{\vec{E}_h \in X_0^h;\ \mathrm{rot}\,\vec{E}_h=\vec{0}\}=\{\mathrm{grad}\,q_h \quad \text{for some} \quad q_h \in Y_0^h\}\ . \tag{15}$$

Besides the tetrahedron element given here, we can also use a rectangular parallelepiped element and a triangular prismatic one (Fig. 1). The explicit expressions of approximate functions for such 3-D edge elements are given in Appendix, together with those for some 2-D edge elements. The convergence of the present approach is discussed in [11, 13] under some assumptions on Ω and triangulations, but we omit the details here.

It is also possible to construct a mixed finite element scheme based on [H2] by the use of subspaces X^h and Y^h in place of X_0^h and Y_0^h. In this case, p_h , the approximation of p in [H2], can be eliminated as in $[\mathrm{E2}]_h$, and we again obtain an approximate problem similar to $[\mathrm{E1}]_h$, in which X^h is used instead of X_0^h. Furthermore, we can finally reduce this problem to the following one expressed by a single equation: Find a pair $\{\lambda_h, \vec{H}_h\} \in \boldsymbol{R}^1 \times X^h$ such that

$$(\mathrm{rot}\,\vec{H}_h, \mathrm{rot}\,\vec{H}_h^*)=\lambda_h(\vec{H}_h, \vec{H}_h^*);\quad \forall \vec{H}_h^* \in X^h\ . \tag{16}$$

When Ω is simply-connected, the eigenspace associated with the zero eigenvalue of (16) is explicitly given by

$$\{\vec{H}_h \in X^h;\ \mathrm{rot}\,\vec{H}_h=\vec{0}\}=\{\mathrm{grad}\,q_h \quad \text{for some} \quad q_h \in Y^h\}\ . \tag{17}$$

Thus, we may solve the cavity resonator problem in terms of $\vec{H}$ by essentially the same finite element procedure as that for the same problem expressed by $\vec{E}$. The difference is only the treatment of boundary conditions.

§ 4. Boundary conditions

The boundary condition to deal with in numerical computations based on $[\mathrm{E2}]_h$ is: $\vec{n}\times\vec{E}=\vec{0}$ on $\partial\Omega$. Thus the only thing required is specifying the edge values of $\vec{E}$ as zero when the corresponding edges are on $\partial\Omega$. Of course, it is practically very combersome to manually prepare input data for boundary edgds, and hence we should design computer programs so that they may automatically identify the edges on $\partial\Omega$. This may be easily done if we notice the fact that any face of an tetrahedron is never shared by two tetrahedra

provided that the face is on $\partial\Omega$.

When we employ finite element schemes based on $[\mathrm{H2}]_h$, we need not consider any boundary conditions in numerical computations, since the imposed boundary conditions are all dealt with as either a natural boundary condition or a constraint condition relaxed by the Lagrange multiplier method.

Besides such physical boundary conditions, we should also consider artificial ones such as arise when Ω has symmetry with respect to a plane. Then the eigenfunctions are expected to be either symmetric or antisymmetric with respect to this plane, and hence we can halve the domain to be analyzed if we can introduce appropriate boundary conditions on this plane.

Let the plane of symmetry be $z=0$ without loss of generality. Then the symmetric and antisymmetric conditions are respectively given by:

(i) **Symmetric condition:** the z-component of a vector function is zero. Hence this condition is the same as $\vec{H}\cdot\vec{n}=0$ in (2), and may be dealt with as a constraint condition relaxed by the Lagrange multiplier method.

(ii) **Antisymmetric condition:** x- and y-components of a vector function are zero, and hence this condition is the same as $\vec{E}\times\vec{n}=\vec{0}$ in (1). Such a condition may be also built into the function space for the vector functions.

Finally, we should notice that the introduction of the above type artificial boundary conditions is usually accompanied with the appearance of interfaces on $\partial\Omega$ where types of boundary conditions change. To express such *mixed* boundary conditions rigorously, we must prepare some special function spaces other than those given in Section 2. The analysis of such function spaces is probably complicated as may be seen from the analysis in [4] of the first-order Sobolev spaces.

§ 5. Problems on axisymmetric domains

It is of special practical interest to consider the case where Ω is an axisymmetric domain. Then, by the *Fourier expansion* technique, we can analyze the problem as a two-dimensional one, for which the use of the two-dimensional Nedelec elements [17, 18] is effective.

When Ω is of axisymmetric shape, we first introduce the cylindrical coordinates $\{r, \theta, z\}$, and consider p and the physical components $\{E_r, E_\theta, E_z\}$ of $\vec{E}$. Then, by the Fourier expansion in θ-direction and taking advantage of the orthogonality of trigonometric functions, we can consider the following sets of functions independently for each $n=0, 1, 2, \cdots$:

$$E_r \sin n\theta, \quad E_\theta \cos n\theta, \quad E_z \sin n\theta, \quad p \sin n\theta\ , \tag{18–1}$$

$$E_r \cos n\theta, \quad E_\theta \sin n\theta, \quad E_z \cos n\theta, \quad p \cos n\theta\ . \tag{18–2}$$

Here we use the same notations E_r, E_θ, E_z and p as before, but the present ones are now functions of r and z only (i.e., independent of θ). Thus our problem becomes two-dimensional. It is also to be noted that the above two sets are in a sense equivalent to each other for $n\geq 1$, and it is sufficient to

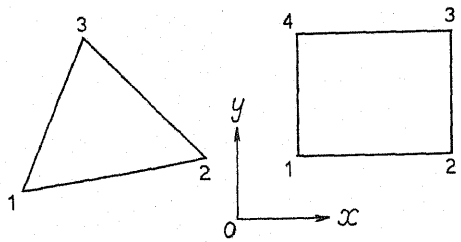

Fig. 2. 2-D edge elements with vertex numberings

consider only one of them except for $n=0$. It is also possible to employ $\vec{H}$ as the fundamental unknown function instead of $\vec{E}$ by essentially the same fashion as will be explained below.

As finite elements for E_r and E_z above, we can use the triangular and rectangular elements proposed by Nedelec [17, 18], see Fig. 2. That is, E_r and E_z are approximated by incomplete linear polynomials in each element. On the other hand, we use the *covariant* compoent $e_\theta=rE_\theta$ instead of the physical component E_θ itself to approximate the θ-component of $\vec{E}$ except for $n=0$. Then e_θ (or E_θ for $n=0$) as well as p are approximated by the piecewise linear polynomial and the piecewise bilinear one respectively in the cases of the triangular and rectangular elements. This choice is effective to assure (11) in the present axisymmetric cases, and hence we can again eliminate p in actual computations. For general curvilinear (not necessarily orthogonal) coordinate systems, the use of covariant components of vectors (or differential 1-form, equivalently) is effective to approximate vector functions in $H(\mathrm{rot}, \Omega)$. The datails may be found in [14], but it is also to be emphasized here that the expression of $\mathrm{rot}\,\vec{E}$ becomes simpler than that in terms of the physical components. For example, in the present cylindrical coordinate case, the physical components of $\mathrm{rot}\,\vec{E}$ are given by [16]:

$$\mathrm{rot}\,\vec{E}=\left\{\frac{1}{r}\left(\frac{\partial E_z}{\partial\theta}-\frac{\partial e_\theta}{\partial z}\right),\ \frac{\partial E_r}{\partial z}-\frac{\partial E_z}{\partial r},\ \frac{1}{r}\left(\frac{\partial e_\theta}{\partial r}-\frac{\partial E_r}{\partial\theta}\right)\right\}. \tag{19}$$

The integration required to calculate the element matrices is, however, slightly more complicated than in the purely 3-D cases. This is mainly due to the $1/r$ factor appearing in the expression of $\mathrm{rot}\,\vec{E}$ in the axisymmetric coordinates. Moreover, some terms in the integrals may diverge to infinity when the considered element has a vertex on the axis of revolution $r=0$, because $\log r$ terms appear in indefinite integrals for $1/r$ terms. We used the formulas given in [21] to compute the integrals exactly expect for the above divergent cases. Furthermore, the infinite terms are approximated by appropriate large numbers such as 10^{10}. That is, we employ a kind of penalty approach to deal with the singularity at $r=0$. Along the axis of revolution, we should impose some conditions on $\vec{E}$ and p, which are given by

$$E_\theta=0 \text{ for } n=0;\quad e_\theta=E_z=p=0 \text{ for } n\geq 1\,. \tag{20}$$

Notice here that these conditions differ with n. Furthermore, some additional conditions are necessary to deal with the singularity at $r=0$: otherwise, the approximation of $\vec{E}$ may not belong to $H(\mathrm{rot}, \Omega)$. Unfortunately, such conditions are difficult to deal with strictly in numerical computations. This is the main reason why we use the penalty approach explained above. At present, the validity of such an approach is not shown theoretically, but we can still check it by numerical tests to a certain extent.

§ 6. Computer programs

Since our problem is three-dimensional, it is absolutely necessary to prepare mesh generator programs even for very simple problems. The essential difference of the Nedelec elements from the usual "vertex" elements is the use of edges as nodes, and this fact must be taken into account in the design of computer codes. In particular, the orientation of edges must be uniquely specified before the assemblage process of element matrices.

We should choose appropriate methods for eigenvalue analysis of the arising algebraic eigenvalue problems. Here we employ the standard subspace iteration method with shift techniques [2]. As we have already mentioned, the use of the shift techniques is essential in our problem since the zero-eigenvalue is highly degenerate in general. As the solver for the linear simultaneous equations appearing in the subspace iteration process, we can use the skyline method [2]. An alternative is proposed by Iwashita [10]: his approach is based on the use of CG (conjugate gradient) method combined with the zero-filtering process, which avoids the use of direct methods such as the skyline method. This approach appears to be very promising especially for 3-D analysis. Moreover, to solve small eigenvalue problems arising from the projection of the original eigenequations to the subspaces, we can use, for example, the classical Jacobi method after using the Cholesky decomposition to the projected mass matrices [2]. Of course, the generalized Jacobi method is also available for the same purposes [2].

In our developed programs, the rectangular parallelepiped element and the triangular prism one are also available. It should be emphasized that our programs can deal with both $[E2]_h$ and $[H2]_h$ just by changing input data for boundary conditions. The deletion procedure for elements is also convenient for 3-D analysis, and is available in our codes. Such utility is actually used in an example given in Section 7. Moreover, the SCG (scaled CG) method is employed as the linear equation solver for the subspace iteration process. This is the simplest possible version of the preconditioned CG methods (PCCG), in which only the diagonal elements of coefficient matrices are used for scaling as a kind of preconditioning.

§ 7. Numerical results

We obtain a few numerical results by the developed computer programs

based on the present theory. Some 2-D examples and more practical 3-D results are respectively reported in [11] and [9].

7.1. Cubic cavity

First, we consider a cubic cavity with unit edge length. In this case, exact eigenpairs are known [1], and we obtain numerically several eigenvalues to see the accuracy of our method. Both E- and H-formulations are tested for all the three types of elements. The domain is divided into $N\times N\times N$ small cubes, and the Friedrichs-Keller type uniform subdivisions are used for the tetrahedron and triangular prism elements. The results for the first three approximate eigenvalues are given in Table 1 for various values of N. Note that the first exact eigenvalue is three-fold degenerate in the present case. Thus the first three approximate eigenvalue denoted by λ_1, λ_2 and λ_3 in the table must coincide with each other in the case of the exact solution. The

Table 1. First three approximate eigenvalues (cubic cavity)
Exact: $\lambda_1=\lambda_2=\lambda_3=2\pi^2=19.739...$
Element type: T=tetrahedron, TP=triangular prism
RP=rectangular parallelepiped

unknown		$\vec{E}$			$\vec{H}$		
element		T	TP	RP	T	TP	RP
N= 1	λ_1	20.000	—	—	23.912	24.000	24.000
	λ_2	—	—	—	23.912	24.000	24.000
	λ_3	—	—	—	24.000	24.000	24.000
N= 2	λ_1	17.064	20.808	24.000	20.731	20.823	24.000
	λ_2	19.643	21.600	24.000	20.731	23.715	24.000
	λ_3	19.643	32.000	24.000	20.819	23.715	24.000
N= 3	λ_1	18.431	20.161	21.600	20.227	20.281	21.600
	λ_2	20.025	20.589	21.600	20.227	21.521	21.600
	λ_3	20.025	25.376	21.600	20.287	21.523	21.600
N= 4	λ_1	18.962	19.962	20.773	20.026	20.059	20.773
	λ_2	19.944	20.217	20.773	20.026	20.744	20.773
	λ_3	19.944	22.866	20.773	20.060	20.745	20.773
N= 5	λ_1	19.226	19.877	20.397	19.926	19.948	20.397
	λ_2	19.880	20.045	20.397	19.926	20.383	20.397
	λ_3	19.880	21.722	20.397	19.948	20.384	20.397
N= 6	λ_1	19.376	19.833	20.194	19.870	19.886	20.194
	λ_2	19.840	19.951	20.194	19.870	20.187	20.194
	λ_3	19.840	21.109	20.194	19.886	20.187	20.194
N= 8	λ_1	19.530	19.791	19.994	19.814	19.823	19.994
	λ_2	19.797	19.858	19.994	19.814	19.992	19.994
	λ_3	19.797	20.506	19.994	19.822	19.992	19.994
N=10	λ_1	19.604	19.772	19.902	19.787	19.733	19.902
	λ_2	19.776	19.815	19.902	19.787	19.901	19.902
	λ_3	19.776	20.228	19.902	19.792	19.901	19.902

accuracy of the numerical results is not fully satisfactory for coarse meshes, but is improved as the mesh becomes finer. To see this more clearly, the errors of the approximate eigenvalues are plotted versus N in $1/N^2$ scale in Fig. 3 in the case of the rectangular parallelepiped element. We can see that the errors are almost proportional to $1/N^2$ for larger values of N, and this phenomenon is fairly commonly observed in lower order elements like the present one when the exact eigenfunctions are sufficiently smooth.

As a reference for evaluating computing time, Table 2 summarizes CPU

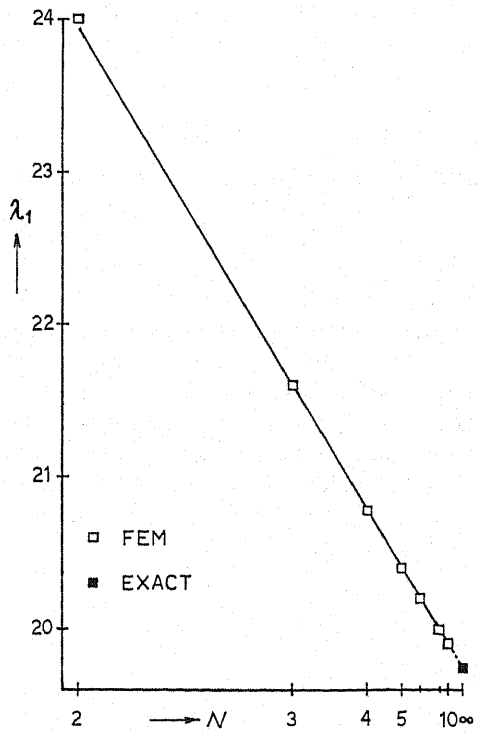

Fig. 3. Convergence plot of the first approximate eigenvalues by the rectangular parallelepiped element (cubic cavity)

Table 2. CPU times for some computers (cubic cavity)

Computer	CPU time
A	460 min.
B	544 sec.
C	513 sec.
C′	452 sec.
D	234 sec.

times for several kinds of supercomputers as well as a personal computer. In the table, $\{A, B, C, D\}$ is a certain permutation of {NEC SX-2, FACOM VP-200, CRAY X-MP/18, NEC PC-9801 RA5}, and C' is C with automatic vectorization. In these personal and supercomputings, the rectangular parallelepiped element is used with $N=10$ for approximating $\bar{E}$ (E-formulation), the dimension of the subspace is 6, the number of obtained eigenpairs is 3, the shift value for Iwasaki's method is 10, the zero-filtering is performed each 2 steps of subspace iteration, and the tolerance of iteration for relative differences of required eigenvalues is chosen 10^{-8}. Moreover, the corresponding calculations with $N=20$ can be performed in about 1 hr., provided that any one of the above supercomputers is used. Thus, this type of 3-D computations are now feasible for practical design purposes if appropriate engineering modeling is introduced.

7.2. Cubic bavity with a half-size cube deleted

Secondly, we consider a unit cubic cavity with a half-size cube deleted as is shown in Fig. 4. We employ the same type of meshes as those in the preceding example, and we utilize the deletion technique installed in the developed code. In this case, no explicit expression is available for the exact solutions. The results are summarized in Table 3 for the first three approximate eigenvalues. The accuracy of the numerical solution is not satisfactory since the present domain has a reentrant corner and the eigenfunctions may have strong singularity there. Still, the results appears to be convergent, and we may conjecture that the first eigenvalue is now simple (non-degenerate) and the second one is two-fold degenerate. Figure 5 shows the mesh ((a): $N=10$) and the vector plots for the surface distributions of the electric and magnetic fields ((b) and (c)) corresponding to the first eigenvalue obtained by the use of the rectangular parallelepiped element.

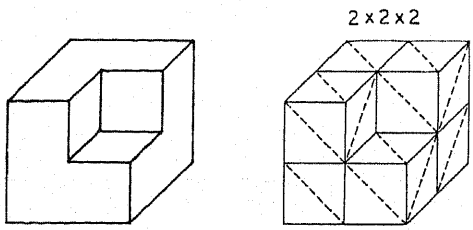

Fig. 4. Cubic cavity with a half-size cube deleted and an example of mesh pattern ($N=2$)

7.3. Circular cylindrical cavity

Using the developed axisymmetric code, we analyze a circular cylindrical cavity of unit radius with height=2. Due to the symmetry of the problem, we analyze only the upper half of the domain, and we partition the cross-section into uniform Friedrichs-Keller type meshes. Examples of meshes are pictured in Fig. 6, where A and B denote two possible directions of diagonals

Table 3. First three approximate eigenvalues (cubic cavity with a half-size cube deleted)
Element type: T=tetrahedron, TP=triangular prism
RP=rectangular parallelepiped

unknown		$\vec{E}$			$\vec{H}$		
element		T	TP	RP	T	TP	RP
N= 2	λ_1	8.0348	11.257	12.000	15.187	16.588	17.368
	λ_2	23.561	27.215	30.000	22.990	25.543	28.207
	λ_3	25.394	36.613	30.000	23.737	27.280	28.207
N= 4	λ_1	10.838	12.207	12.420	13.814	14.222	14.166
	λ_2	23.514	24.295	25.020	23.507	24.106	24.786
	λ_3	23.920	26.577	25.020	23.658	24.850	24.786
N= 6	λ_1	11.676	12.449	12.567	13.425	13.648	13.549
	λ_2	23.330	23.869	24.184	23.505	23.787	24.082
	λ_3	23.698	24.863	24.184	23.575	24.140	24.082
N= 8	λ_1	12.055	12.566	12.646	13.253	13.401	13.310
	λ_2	23.406	23.721	23.896	23.502	23.670	23.835
	λ_3	23.619	24.278	23.896	23.543	23.875	23.835
N=10	λ_1	12.266	12.635	12.696	13.158	13.266	13.188
	λ_2	23.444	23.652	23.763	23.502	23.615	23.720
	λ_3	23.583	24.009	23.763	23.529	23.750	23.720
N=20	λ_1	—	—	12.797	—	—	12.993
	λ_2	—	—	23.584	—	—	23.569
	λ_3	—	—	23.584	—	—	23.569

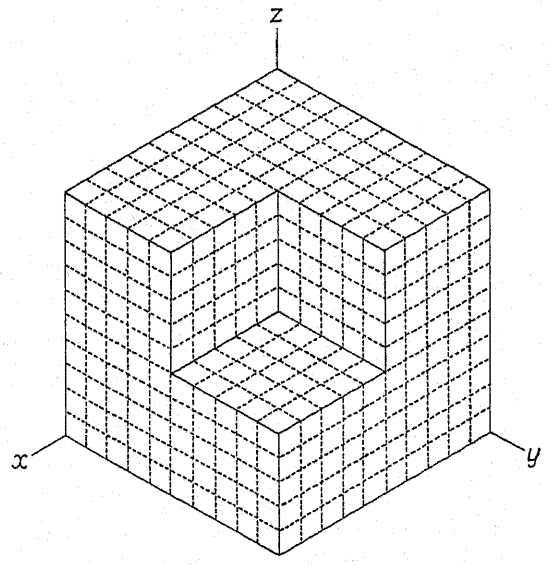

Fig. 5(a). Vector plots of the approximate first eigenfunction (N=10) : mesh

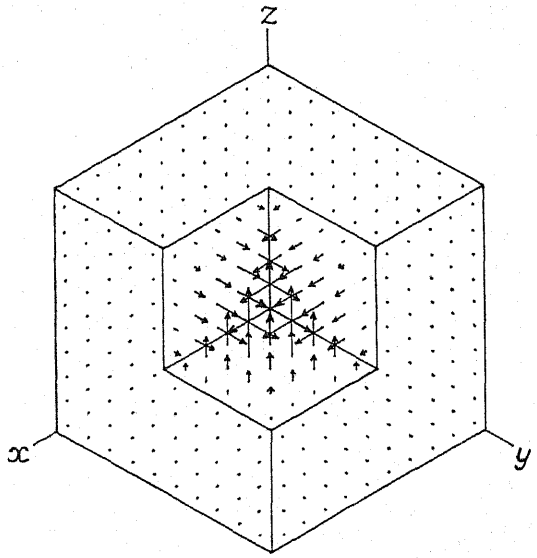

Fig. 5(b). Vector plots of the approximate first eigenfunction (N=10) : $\vec{E}$

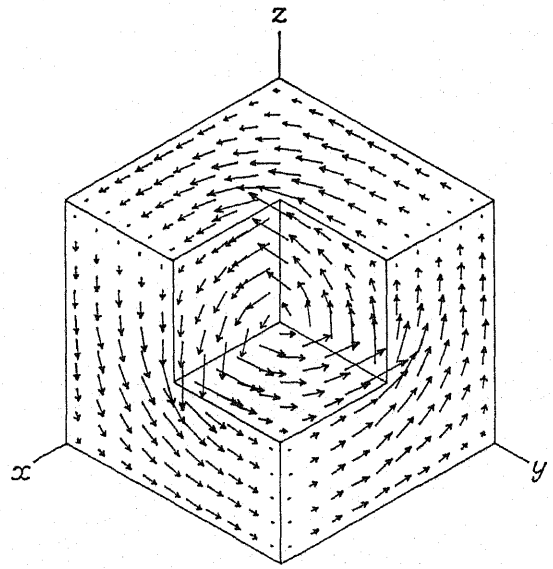

Fig. 5(c). Vector plots of the approximate first eigenfunction (N=10) : $\vec{H}$

of small rectangles in the meshes. Both triangular and rectangular elements are tested. As is discussed in section 4, symmetric or antisymmetric conditions must be taken into account on the plane of symmetry z=0. In this case, exact

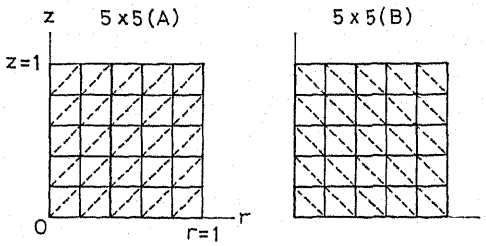

Fig. 6. Examples of mesh patterns for the axisymmetric domain (upper half portion)

Table 4. First three approximate eigenvalues (circular cylindrical cavity)

mode & unknown		triangle				rectangle		exact
		5×5*A*	5×5*B*	10×10*A*	10×10*B*	5×5	10×10	
TM_{010}	$\vec{E}$	5.6861	5.6861	5.7588	5.7588	5.8016	5.7882	5.7832
	$\vec{H}$	5.8377	5.8377	5.7970	5.7970	5.8389	5.7970	
TE_{111}	$\vec{E}$	6.0569	6.1001	5.9101	5.9222	5.9501	5.8796	5.8574
	$\vec{H}$	6.1705	6.2240	5.9441	5.9546	5.8978	5.8675	
TM_{011}	$\vec{E}$	8.2442	8.2013	8.2489	8.2383	8.2894	8.2607	8.2506
	$\vec{H}$	8.3469	8.3720	8.2752	8.2810	8.3267	8.2695	

solutions are obtainable by the use of the Bessel functions [1], and can be effectively used for the comparison with approximate solutions.

Table 4 summarizes the first three approximate eigenvalues of the present problem. The corresponding modes are called TM_{010}, TE_{111}, and TM_{011} [1]: the first and the third modes are axisymmetric ones, while the second is not axisymmetric and the associated n in (18) is unity. The results are generally reasonable for both E- and H-formulations, but those for TE_{111} are slightly poor in accuracy probably because of the insufficient approximation capability of the present method near the axis of revolution $r=0$.

§ 8. Concluding remarks

We have proposed a mixed finite element method for 3-D analysis of cavity resonators. We have also presented some axisymmetric finite element models, where the distributions of fields can vary in θ-direction. In both cases, the use of the Nedelec elements for $H(\mathrm{rot}, \Omega)$ is essential. We also tested the method numerically by very primitive examples. It is of course important to apply the method to more practical problems as well as to develop efficient computer programs by improving numerical techniques. Moreover, the use of mixed finite element methods also appears to be promising for electrostatic and magnetostatic problems. Finally, it is to be pointed out that there remain

various unsolved theoretical problems related to the validity of our approach, as may be seen from the descriptions of this paper.

The contents of this paper was partially presented as an invited talk of IMACS/IFAC International Symposium on Modelling and Simulation of Distributed Parameter Systems held in Hiroshima on October 6-9 in 1987.

ACKNOWLEDGEMENTS. The authors wish to thank Dr. M. Okebe of Optopian Corp. for his valuable comments on interpolation functions of edge elements and quadrature formulas over axisymmetric regions. They also appreciate much Mr. M. Hashimoto of NEC Corp. and Mr. K. Ishii of Quint Corp. for their cooperation in supercomputings related to this work.

Appendix. Interpolation functions for edge elements

In this Appendix, we give explicit expressions of approximate vector-valued functions for several types of 2-D and 3-D Nedelec (edge) elements shown in Figs. 1 and 2 with their vertex numberings. In what follows, Ω_e denotes a finite element, integer i any one of the vertices of Ω_e, $\vec{ij}$ the vector representing the edge from vertex i to j, l_{ij} the length of $\vec{ij}$, and E_{ij} the projection of the approximate vector-valued function $\vec{E}_h$ to the edge $\vec{ij}$. Moreover, $\{x_i, y_i\}$ (2-D cases) or $\{x_i, y_i, z_i\}$ (3-D cases) are cartesian coordinates of vertex i.

A1. Triangular element

Let Ω_e be a triangle with vertices indicated in Fig. 2. We denote by $\{i, j, k\}$ any one of the cyclic (even) permutations of $\{1, 2, 3\}$. Then the explicit expression of $\vec{E}_h$ in each Ω_e is given by

$$\vec{E}_h=\begin{pmatrix}E_{hx}\\E_{hy}\end{pmatrix}=\sum_{\{i,j,k\}}\frac{E_{ij}l_{ij}}{D}\begin{pmatrix}y_k-y\\x-x_k\end{pmatrix}, \tag{A1}$$

where D is the determinant defined by

$$D=\begin{vmatrix}1 & x_i & y_i\\1 & x_j & y_j\\1 & x_k & y_k\end{vmatrix}. \tag{A2}$$

The value of D is actually independent of the choices of $\{i, j, k\}$. Another explicit form of expression is given by Bossavit [3] in terms of barycentric coordinates.

A2. Rectangular element

Let Ω_e be a rectangle with vertices indicated in Fig. 2. The edges of Ω_e are assumed to be parallel to one of the coordinate axes. The components of $\vec{E}_h=\{E_{hx}, E_{hy}\}$ in Ω_e are given by

$$E_{hx}=E_{12}(1-Y)+E_{43}Y\,,\quad E_{hy}=E_{14}(1-X)+E_{23}X\,, \tag{A3}$$

where

$$X=(x-x_1)/(x_2-x_1)\ ,\quad Y=(y-y_1)/(y_4-y_1)\ . \tag{A4}$$

A3. Tetrahedron element

Let Ω_e be a tetrahedron with vertices indicated in Fig. 1. We denote by $\{i, j, k, m\}$ any one of the permutations of $\{1, 2, 3, 4\}$ defined in Table 5. Then the explicit expression of $\vec{E}_h$ in Ω_e is given by

Table 5. Node numberings for the tetrahedron element

Case	i	j	k	m
1	1	2	3	4
2	1	3	4	2
3	1	4	2	3
4	2	3	1	4
5	2	4	3	1
6	3	4	1	2

$$\vec{E}_h=\begin{pmatrix} E_{hx} \\ E_{hy} \\ E_{hz} \end{pmatrix}$$

$$=\sum_{\{i,j,k,m\}}\frac{E_{ij}l_{ij}}{D}\begin{pmatrix} (z_k-z_m)y+(y_m-y_k)z+y_kz_m-y_mz_k \\ (z_m-z_k)x+(x_k-x_m)z+x_mz_k-x_kz_m \\ (y_k-y_m)x+(x_m-x_k)y+x_ky_m-x_my_k \end{pmatrix}\ , \tag{A5}$$

where D is the determinant defined by

$$D=\begin{vmatrix} 1 & x_i & y_i & z_i \\ 1 & x_j & y_j & z_j \\ 1 & x_k & y_k & z_k \\ 1 & x_m & y_m & z_m \end{vmatrix}\ . \tag{A6}$$

Actually, the value of D is independent of the choices of $\{i, j, k, m\}$. Another explicit expression is given by Bossavit [3].

A4. Rectangular parallelepiped element

Let Ω_e be a rectangular parallelepiped with vertices indicated in Fig. 1. The edges of Ω_e are assumed to be parallel to one of the coordinate axes. The components of $\vec{E}_h=\{E_{hx}, E_{hy}, E_{hy}\}$ in Ω_e are given by

$$\begin{aligned} E_{hx}&=E_{12}(1-Y)(1-Z)+E_{43}Y(1-Z)+E_{87}YZ+E_{56}(1-Y)Z\ , \\ E_{hy}&=E_{14}(1-Z)(1-X)+E_{58}Z(1-X)+E_{67}ZX+E_{23}(1-Z)X\ , \\ E_{hz}&=E_{15}(1-X)(1-Y)+E_{26}X(1-Y)+E_{37}XY+E_{48}(1-X)Y\ , \end{aligned} \tag{A7}$$

where

$$X=(x-x_1)/(x_2-x_1)\ ,\quad Y=(y-y_1)/(y_4-y_1)\ ,\quad Z=(z-z_1)/(z_5-z_1)\ . \tag{A8}$$

A5. Triangular prism element

Let Ω_e be a triangular prism with vertices indicated in Fig. 1. Its top and bottom surfaces are assumed to be parallel to $x-y$ plane, while its side surfaces to be parallel to z-axis. We denote by $\{i, j, k\}$ any one of the cyclic permutations of $\{1, 2, 3\}$. The components of $\vec{E}_h=\{E_{hx}, E_{hy}, E_{hz}\}$ in Ω_e are given by

$$\begin{aligned} E_{hx}&=\sum_{\{i,j,k\}} l_{ij}(y_k-y)\{E_{ij}(1-Z)+E_{i+3,j+3}Z\}/D\ ,\\ E_{hy}&=\sum_{\{i,j,k\}} l_{ij}(x-x_k)\{E_{ij}(1-Z)+E_{i+3,j+3}Z\}/D\ ,\\ E_{hz}&=\sum_{i=1}^{3} E_{i,i+3}L_i\ , \end{aligned} \tag{A9}$$

where

$$D=\begin{vmatrix} 1 & x_i & y_i \\ 1 & x_j & y_j \\ 1 & x_k & y_k \end{vmatrix}\ ,\quad Z=(z-z_1)/(z_4-z_1)\ , \tag{A10}$$

$$L_i=x_jy_k-x_ky_j+(y_j-y_k)x+(x_k-x_j)y\ .$$

Notice here that L_i's for $1\leq i\leq 3$ are nothing but the area coordinates over the triangle of the bottom surface $\{1, 2, 3\}$ or the top surface $\{4, 5, 6\}$.

References

[1] Atwater, H. A., *Introduction to microwave theory*, McGraw-Hill, 1962.

[2] Bathe, K.-J., and Wilson, E. L., *Numerical methods in finite element analysis*, Prentice-Hall, 1976.

[3] Bossavit, A., Calcul des courants induits et des forces électromagnétiques dans un système de conducteurs mobiles, *Math. Model. & Numer. Anal.*, **23** (1989), 235–259.

[4] Doktor, P., On the density of smooth functions in certain subspaces of Sobolev spaces, *Comment, Math. Univ. Carolinae*, **14** (1973), 609–622.

[5] Duvaut, G., and Lions, J. L., *Inequalities in mechanics and physics*, Springer, 1967, Ch. 7.

[6] Girault, V., and Raviart, P.-A., *Finite element methods for Navier-Stokes equations, theory and algorithms*, Springer, 1986, Ch. 1.

[7] Gruber, R., and Rappaz, J., *Finite element methods in linear ideal magnetohydrodynamics*, Springer, 1985, Chs. 1 & 7.

[8] Hano, M., Finite-element analysis of dielectric-loaded waveguides, *IEEE Trans. Microwave Theory & Tech.*, **MTT-32** (1984), 1275–1279.

[9] Hara, M., Wada, T., Mitomori, K., and Kikuchi, F., Three dimensional analysis of RF electromagnetic field by the finite element method, in *Proc. 11-th Int. Conf. Cyclotron and their Applications, Oct. 13–17, 1986, Tokyo* (*M. Sekiguchi, Y. Yano, and K. Hatanaka, Eds.*), IONICS Pub. Co. (1987), 337–340.

[10] Iwashita, Y., General eigenvalue solver for large sparse symmetric matrix with zero filtering, *Bull. Inst. Chem. Res., Kyoto Univ.*, **67** (1989), 32–39.

[11] Kikuchi, F., Mixed and penalty formulations for finite element analysis of an eigenvalue problem in electromagnetism, *Computer Meth. Appl. Mech. Eng.*, **64** (1987), 509–521.

[12] Kikuchi, F., Weak formulations for finite element analysis of an electromagnetic eigenvalue problem, *Sci. Papers Coll. Arts & Sci., Univ. Tokyo*, **38** (1988), 43–67.

[13] Kikuchi, F., On a discrete compactness property for the Nedelec finite elements, *J. Fac. Sci., Univ. Tokyo, Sec. IA*, **36** (1989), 479–490.

[14] Kikuchi, F., Covariant and contravariant finite elements for Sobolev-like spaces, to appear.

[15] Krizek, M., and Neittaanmaki, P., *Finite element approximation of variational problems and applications*, Longman Scientific & Technical, 1990, Chs. 12 & 13.

[16] Morse, P. M., and Feshbach, H., *Methods of theoretical physics, Part I*, McGraw-Hill, 1953, Ch. 1.

[17] Nedelec, J.-C., Mixed finite elements in $\boldsymbol{R}^3$, *Numer. Math.*, **35** (1980), 315–341.

[18] Nedelec, J.-C., A new family of mixed finite elements in $\boldsymbol{R}^3$, *Numer. Math.*, **50** (1986), 57–81.

[19] Weiland, T., A discretization method for the solution of Maxwell's equations and applications for six-component fields, *AEU*, **31** (1977), 116–120.

[20] Whitney, H., *Geometric integration theory*, Princeton Univ. Press, 1957.

[21] Zienkiewicz, O. C., and Cheung, Y. K., *The finite element method in structural and continuum mechanics*, McGraw-Hill, 1967, Ch. 4.